Scan-Specific Residual Convolutional Neural Networks for Fast MRI Using Residual RAKI

Chi Zhang*,†, Seyed Amir Hossein Hosseini*,†, Steen Moeller†, Sebastian Weingärtner*,†,‡, Kâmil Uğurbil† and Mehmet Akçakaya*,†

* Department of Electrical and Computer Engineering, University of Minnesota, Minneapolis, MN

† Center for Magnetic Resonance Research, University of Minnesota, Minneapolis, MN

‡ Department of Imaging Physics, Delft University of Technology, Delft, Netherlands

Emails: {zhan4906, hosse049, moell018, sweingae, ugurb001, akcakaya}@umn.edu

***Abstract*—Parallel imaging is a widely-used acceleration technique for magnetic resonance imaging (MRI). Conventional linear reconstruction approaches in parallel imaging suffer from noise amplification. Recently, a non-linear method that utilizes subject-specific convolutional neural networks for k-space reconstruction, Robust Artificial-neural-networks for k-space Interpolation (RAKI) was proposed and shown to improve noise resilience over linear methods. However, the linear convolutions still provide a sufficient baseline image quality and interpretability. In this paper, we sought to utilize a residual network architecture to combine the benefits of both the linear and non-linear RAKI reconstructions. This hybrid method, called residual RAKI (rRAKI) offers significant improvement in image quality compared to linear method, and improves upon RAKI in highly-accelerated simultaneous multi-slice imaging. Furthermore, it establishes an interpretable view for the use of CNNs in parallel imaging, as the CNN component in the residual network removes the noise amplification arising from the linear part.**

I. Introduction

Long scan times remain a challenge in magnetic resonance imaging (MRI). Several methods exist for accelerating MRI scans by undersampling the acquisitions beyond Nyquist rate, and reconstructing these using additional information. Parallel imaging is the most commonly used accelerated MRI method [1]–[3]. These methods use differences in the profiles of multiple receiver coils for reconstruction [1]. These differences are estimated from scan-specific calibration data [2], [3], after which the reconstruction is performed either as an inverse problem in image domain [2] or an interpolation problem in k-space [3].

These reconstruction strategies are linear in nature. Therefore, at higher undersampling rates or low signal-to-noise ratio (SNR) regimes, they suffer from noise amplification [2], [3]. Thus, several alternative strategies have been proposed. More recently, machine learning (ML) techniques have been explored to improve the reconstruction quality with several promising studies [5]–[17]. However, these methods require large databases of training data, containing fully-sampled images. Such training data is not always available practice, especially when spatio-temporal resolution is important, such as in cardiac MRI. Furthermore, the training datasets may not include sufficiently many pathologies of interest. Consequently, database-trained deep learning methods incur risks in generalizability for diagnosis [18], which may hinder their clinical application.

An alternative line of work in ML reconstruction for MRI is scan-specific reconstruction. The first method of this type, Robust Artificial-neural-networks for k-space Interpolation (RAKI) [19] interpolates undersampled k-space using convolutional neural networks (CNNs) trained on scan-specific ACS data. Thus RAKI extends the use of linear convolutional kernels for k-space interpolation in the traditional GRAPPA method [3] to non-linear CNNs with significant gains in noise reduction [19]. The scan-specificity of RAKI comes with benefits in offering robustness to biases in training datasets, such as under-representation of rare pathological features [18], as well as not requiring fully-sampled data for training. This method was also extended to simultaneous multi-slice (SMS) imaging [20] and arbitrary undersampling patterns [21], [22].

Even with the improvements provided by RAKI methods, the source of the improvement is not easy to identify. As interpretable algorithms for ML increasingly become important to reduce the "black-box" stigma associated with such tools [23], [24], it is imperative to provide more interpretable methods in the RAKI framework to facilitate their clinical translation.

In this paper, we combine the advantages of linear GRAPPA and non-linear RAKI reconstructions in an interpretable manner, while maintaining the scan-specificity of RAKI. This new method, called residual RAKI (rRAKI), uses a residual CNN that includes a skip connection incorporating a linear convolution in parallel with a multi-layer CNN. Thus, the linear skip connection implements a linear interpolation similar to GRAPPA, while the multi-layer non-linear CNN estimates the imperfections that arise from the linear component, such as noise amplification. All components in this residual CNN are trained on scan-specific ACS data. Experiments in brain imaging show that rRAKI has noticeable advantages over linear methods in terms of noise resilience and artifact removal. It also produces sharper images compared to RAKI in a challenging highly-accelerated SMS imaging scenario.

II. Methods

A. Background on k-space Interpolation and RAKI

GRAPPA [3] is one of the most clinically-used k-space interpolation methods for parallel imaging. In GRAPPA, a

set of linear shift-invariant convolution kernels are estimated from ACS data. Let R be the acceleration rate with uniform undersampling and n_c be the number of coils. Let $s(k_x, k_y, i)$ denote the k-space point at position (k_x, k_y) in coil i. For notational convenience, let

$$\begin{aligned}\mathcal{N}(k_x, k_y) = \{(k_x - b_x\Delta k_x, k_y - Rb_y\Delta k_y, i) : \\ b_x \in \{-B_x, \ldots, B_x\}, \\ b_y \in \{-B_y, \ldots B_y\}, \\ i \in \{1, \ldots, n_c\}\}\end{aligned} \tag{1}$$

denote a neighborhood of sampled points around the k-space location (k_x, k_y) across all coils, where B_x and B_y are pre-specified integer-valued kernel sizes. We define $\tilde{\mathbf{s}}_{\mathcal{N}(k_x,k_y)}$ be the column vector whose entries are elements $s(a, b, c)$ with $(a, b, c) \in \mathcal{N}(k_x, k_y)$. With this notation, GRAPPA estimates the missing points in a uniformly undersampled k-space acquisition by interpolating the acquired points in its vicinity as:

$$s(k_x, k_y - m\Delta k_y, i) = \mathbf{g}_{m,i}\tilde{\mathbf{s}}_{\mathcal{N}(k_x,k_y)}, \tag{2}$$

where $\mathbf{g}_{m,i}$ is a row vector that contains the corresponding linear convolutional weights for estimating the m^{th} skipped line in coil i. The GRAPPA convolution kernel is obtained by solving a linear least squares problem, where the calibration points in the ACS region are used as regressors and regressand in Eq. (2).

GRAPPA suffers from noise amplification at high acceleration rates similar to other linear parallel imaging approaches [2]. RAKI extends this idea of linear convolutions to performing non-linear interpolation using CNNs [19]. This non-linear interpolation strategy was shown to improve upon the noise amplification associated with GRAPPA [19]. Similar to GRAPPA, the CNNs in RAKI are trained from the ACS data. For processing, complex k-space data is mapped to real field, leading to a total of $2n_c$ input channels from n_c coils. This affects the way the neighborhood is defined in Eq. (1), as i now ranges over 1 to $2n_c$. We will use $\tilde{\mathcal{N}}$ to denote this new definition over the real field, and define $\tilde{\mathbf{s}}_{\tilde{\mathcal{N}}(k_x,k_y)}$ analogously. Additionally let

$$\begin{aligned}\mathcal{U}(k_x, k_y, j) = \{(k_x, k_y - m\Delta k_y, j) : \\ m \in \{1, \ldots R-1\}\}\end{aligned} \tag{3}$$

denote the $R-1$ missing phase encoding points adjacent to (k_x, k_y) in channel j. Let $\tilde{\mathbf{s}}_{\mathcal{U}(k_x,k_y,j)}$ denote the column vector whose entries are elements $s(a, b, c)$ with $(a, b, c) \in \mathcal{U}(k_x, k_y, j)$. Then RAKI interpolation estimates the missing k-space points using acquired data via CNNs as:

$$\tilde{\mathbf{s}}_{\mathcal{U}(k_x,k_y,j)} = f_j\big(\tilde{\mathbf{s}}_{\tilde{\mathcal{N}}(k_x,k_y)}\big) \tag{4}$$

where $f_j(\cdot)$ denotes the CNN that uses acquired data to estimate skipped points in channel j. A three-layer CNN was used in [19] for this process. The first two layers consisted of convolutions and point-wise non-linear activation via the rectified linear unit, $\text{ReLU}(x) = \max(x, 0)$, while the last layer of the network only contained convolutions to generate the final estimation.

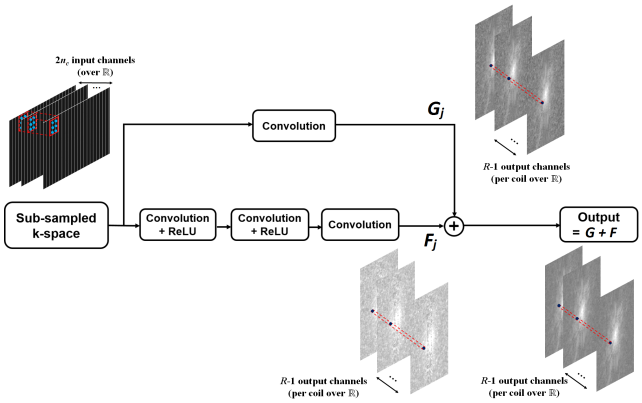

Fig. 1. The proposed residual network architecture used in rRAKI. The input to the network is all the sampled k-space data across all coils, while the output is all missing lines for a given coil, leading to $R-1$ output channels. A linear k-space convolution is implemented via the residual connection, denoted by G_j. A 3-layer network is used for estimating the artifacts arising from this linear part. The architecture of this network is similar to that in RAKI [19], and is denoted by F_j. The final reconstruction combines these two components, $G_j + F_j$.

B. Proposed Residual RAKI (rRAKI)

Figure 1 depicts the proposed residual network architecture [25] used in rRAKI. The input to the network is all sampled data across all channels. The rRAKI network for channel j estimates all the missing lines for that channel. The network itself consists of a a multi-layered CNN F_j, along with a residual connection that implements a linear reconstruction using shift-invariant convolutions in k-space, denoted by G_j. The multi-layered network, F_j non-linearly estimates the residual artifacts arising from the linear reconstruction for that particular scan and compensates for these. Similar to [19], a 3-layered CNN was employed in this study. Thus, the rRAKI reconstruction can be summarized as:

$$\tilde{\mathbf{s}}_{\mathcal{U}(k_x,k_y,j)} = F_j\big(\tilde{\mathbf{s}}_{\tilde{\mathcal{N}}(k_x,k_y)}\big) + G_j\big(\tilde{\mathbf{s}}_{\tilde{\mathcal{N}}(k_x,k_y)}\big) \tag{5}$$

In our implementation, F_j and G_J are trained jointly. Thus, our goal is to enforce the baseline properties of the linear part. Let $\mathbf{y}_j$ denote the target points in ACS region, and $\mathbf{y}_{\text{source}}$ denote the source points in the ACS region [3], [19]. The training loss for channel j network is given by

$$\begin{aligned}\min_{\boldsymbol{\theta}_j} \; & ||\mathbf{y}_j - F_j(\mathbf{y}_{\text{source}}; \boldsymbol{\theta}_j) - G_j(\mathbf{y}_{\text{source}}; \boldsymbol{\theta}_j)||_2^2 \\ & \text{s. t.} \quad ||\mathbf{y}_j - G_j(\mathbf{y}_{\text{source}}; \boldsymbol{\theta}_j)||_2^2 < \delta\end{aligned} \tag{6}$$

where $||\cdot||_2$ denotes the ℓ_2 norm; δ is a scalar that limits the linear reconstruction error. The equivalent unconstrained problem using Lagrangian multipliers is given as

$$\begin{aligned}\min_{\boldsymbol{\theta}_j} \; & ||\mathbf{y}_j - F_j(\mathbf{y}_{\text{source}}; \boldsymbol{\theta}_j) - G_j(\mathbf{y}_{\text{source}}; \boldsymbol{\theta}_j)||_2^2 \\ & + \lambda||\mathbf{y}_j - G_j(\mathbf{y}_{\text{source}}; \boldsymbol{\theta}_j)||_2^2\end{aligned} \tag{7}$$

where λ is a Lagrangian multiplier.

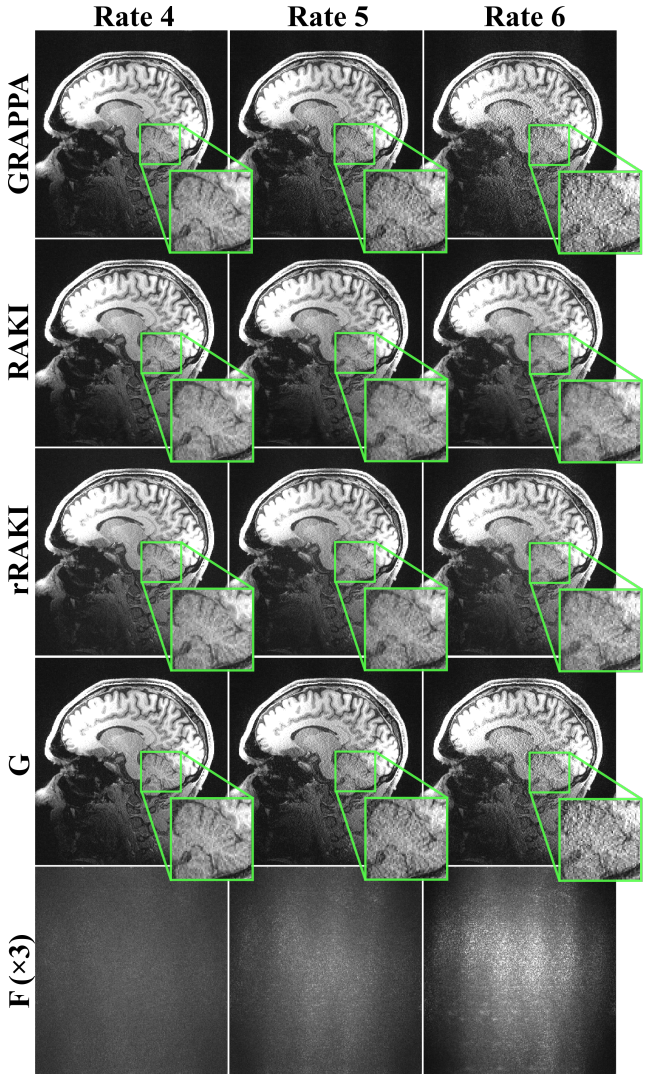

Fig. 2. 3T brain imaging reconstruction results of MPRAGE data (0.7mm isotropic) at R = 4, 5, 6, using GRAPPA, RAKI, rRAKI. GRAPPA suffers from noise amplification at high acceleration rates. Both RAKI and rRAKI demonstrate improvements in noise resilience. The G term in rRAKI is close to linear reconstruction (GRAPPA) result, while the F term estimates coil geometry-based noise amplification. No noticeable blurring artifacts were observed in rRAKI reconstruction at this high resolution.

C. In Vivo Imaging Experiments

Brain imaging was performed using a 3T Siemens Magnetom Prisma (Siemens Healthcare, Erlangen, Germany) systemwith a 32-channel receiver head coil-array. A T_1-weighted 3D-MPRAGE sequence was acquired in a healthy subject (male, 41 years) with the following parameters: FOV = $224\times224\times179\text{mm}^3$, resolution = $0.7\times0.7\times0.7\text{mm}^3$, matrix size = 320×320, TR/TE = 2400 ms/2.2 ms, flip angle = 8°, bandwidth = 210 Hz/pixel, inversion time = 1000 ms, ACS lines = 40, with iPAT = 2 and 5. Furthermore, the R = 2 acquisition was also retrospectively undersampled to R = 4 and 6. The k-space data was inverse Fourier transformed along the slice direction, and a central slice was processed.

SMS fMRI acquisition was performed using the Human Connectome Project protocol [26] at 3T with the following parameters: resolution = $2\times2\times2\text{mm}^3$, using blipped-CAIPI encoding [27] with a field-of-view/3 shift between adjacent multiband slices. Images were acquired using a multiband rate of 16 (MB16) with echo time = 37ms, repetition time = 1000ms. Calibration data containing the individual slices was acquired prior to the fMRI image series at the same resolution. Fully-sampled slices obtained from individual scans were concatenated along the readout direction in image domain to build the subject-specific ACS data used for training of the CNN [28], [29].

For all acquisitions, fully-sampled references were not available, thus reconstructions were assessed qualitatively.

D. Implementation Details

Network parameters in [19] were used for RAKI and the $F_j(\cdot)$ of rRAKI in reconstructions of 3T imaging. For SMS imaging, the network parameters employed in [29] were adopted for both RAKI and $F_j(\cdot)$ of rRAKI. $G_j(\cdot)$ and the first layer of $F_j(\cdot)$ were designed to have the same kernel size. GRAPPA kernel size has been chosen as 5 by 4. According to our experiments, bigger kernels did not improve the final results. In this study, λ was set to 1. Adam optimizer [30] was used for CNN training. For all reconstructions, the final images were generated using the root-sum-of-squares combination of individual coil images. RAKI and rRAKI were implemented using python 3.6.2 and TensorFlow 1.3.0, supported by CUDA 8.0 and CuDNN 7.0.5. Python environment was created by Anaconda 3.8.3. GRAPPA was implemented using Matlab R2016b (MathWorks Inc., Natick, MA).

III. Results

Figure 2 depicts the results of the 3T MPRAGE reconstructions using GRAPPA, RAKI, rRAKI, as well as the linear part of rRAKI, $G(\cdot)$ and the non-linear part of rRAKI, $F(\cdot)$ scaled by a factor of 3 for improved visualization. All three approaches successfully remove the aliasing artifacts. For $R = 4$, RAKI and rRAKI have slightly lower noise than GRAPPA. This advantage of RAKI and rRAKI in noise resilience become more pronounced for acceleration rates of 5 and 6, where RAKI and rRAKI have visually lower noise than GRAPPA. Furthermore, the linear, $G(\cdot)$ part of rRAKI is very close to the GRAPPA results as desired. $F(\cdot)$ shows satisfying ability to reduce the noise amplification from this linear part, leading to the final rRAKI result, which matches that of RAKI in terms of noise resilience.

Figure 3 presents 6 example slices out of 16 simultaneously acquired ones for 3T SMS imaging. Both RAKI and rRAKI show improved noise resilience over GRAPPA. However, rRAKI shows advantages over both RAKI and GRAPPA, by offering sharper images as well as fewer residual artifacts. An SMS acceleration of 16 is a considerably high rate, which leads to substantial noise amplification and residual artifacts for linear reconstructions, including GRAPPA and the linear $G(\cdot)$ component of rRAKI. Note the non-linear component, $F(\cdot)$, captures more than just noise amplification in this case,

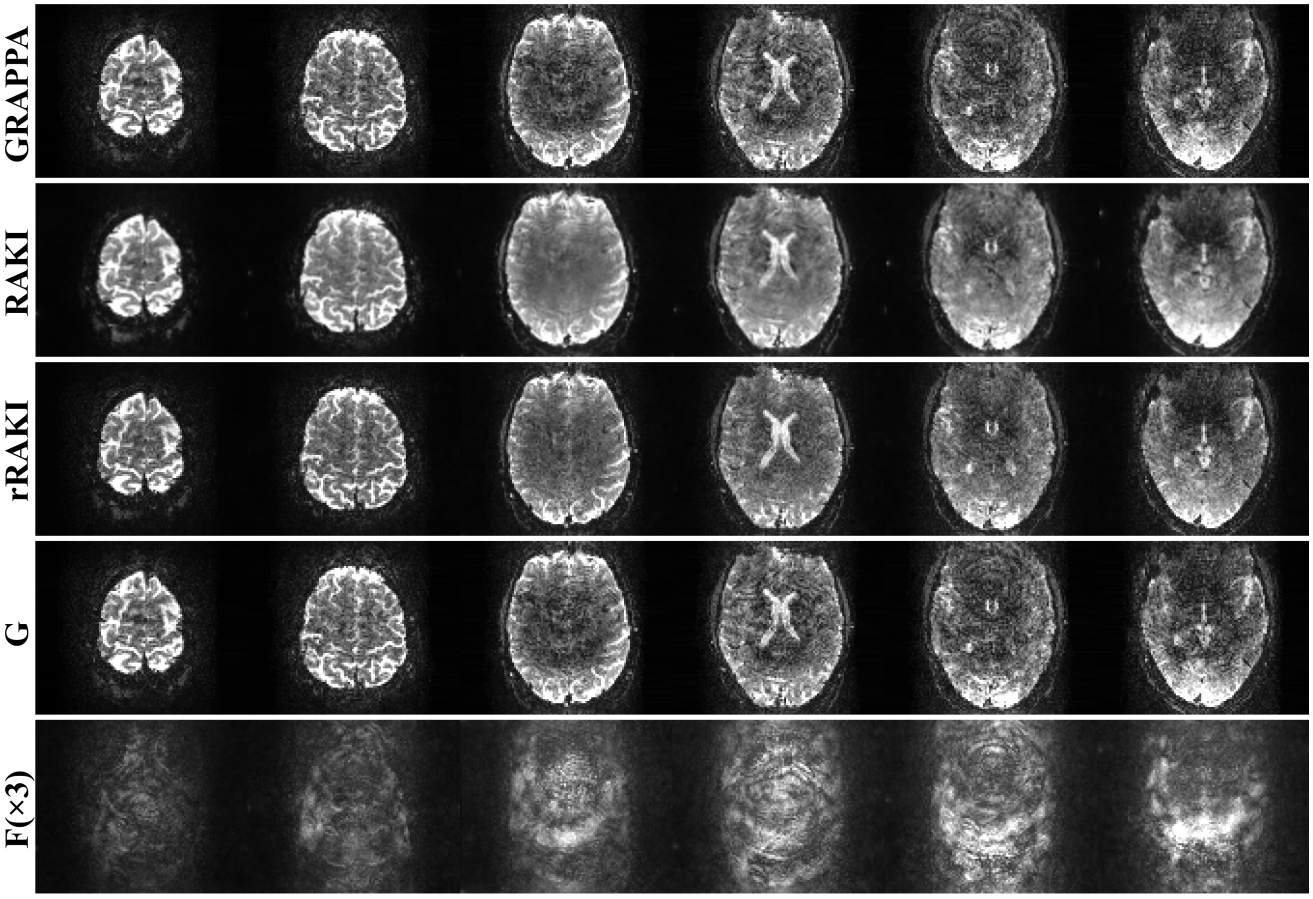

Fig. 3. Six slices from reconstructions of 3T Simultaneous Multi-Slice imaging fMRI data with multi-band acceleration rate = 16. rRAKI outperforms GRAPPA in terms of noise amplification, while showing fewer blurring artifacts compared to RAKI. In addition to noise amplification, F component in rRAKI also captures ghosting artifacts caused by imperfections in the EPI-based ACS data.

due to the imperfections of the EPI-based ACS data for this application.

IV. Discussion

In this work, we proposed an interpretable ML approach for scan-specific accelerateed MRI reconstruction using CNNs. Our method, rRAKI utilized a residual network architecture to interpolate missing k-space lines using both linear and non-linear components, both of which were trained on subject-specific calibration, eliminating the need for a database of images. Our proposed method provided better noise properties than GRAPPA, and fewer blurring artifacts than RAKI.

Different to conventional residual network architectures [25], our architecture featured a skip connection with a linear convolution. This was important for our problem to include a linear reconstruction method as a sub-component, but it also required changes to conventional residual connections. How the benefits of residual networks, such as accelerated convergence and hypothesized easier optimization of the residual mapping, extend to this case warrants further investigation.

In our work, we jointly trained the linear convolutional component and the non-linear part. An alternative approach would have been to fix the GRAPPA kernel following least squares estimation, and use the explicit residual for training at the output without a residual connection in the CNN. However, in our experiments, this led to sub-par performance, often converging to local minima, even when using a batch normalization layer.

Although ML techniques demonstrated superiors outcomes in MRI reconstruction both visually and quantitatively, interpretability is still desirable for clinical adoption of ML methods. rRAKI addresses two issues for clinical translation, including scan-specificity and interpretability. For the former, it avoids the risks caused by insufficient or biased inclusion of rare pathologies in training databases, which may affect other methods [18]. For the latter, the residual architecture provides a linear reconstruction baseline, which matches the linear GRAPPA method, while the non-linear CNN learns the reconstruction residual to mitigate noise and artifacts arising from the linear component. Such interpretability can also be extended to other sampling patterns [21], [22].

V. Conclusion

The proposed residual RAKI method learns a linear reconstruction along with a CNN that removes the artifacts arising from this linear portion for parallel imaging in a scan-specific manner on limited calibration data, and provides improvements upon existing k-space interpolation strategies.

ACKNOWLEDGMENT

This work was partially supported by NIH P41EB015894, NIH U01EB025144, NIH P41EB027061, NSF CAREER CCF-1651825.

REFERENCES

[1] D. K. Sodickson, and W. J. Manning. "Simultaneous acquisition of spatial harmonics (SMASH): fast imaging with radiofrequency coil arrays," *Magn. Reson. Med.*, vol. 38, no. 4, pp. 591-603, 1997.

[2] K. P. Pruessmann, M. Weiger, M. B. Scheidegger and P. Boesiger, "SENSE: sensitivity encoding for fast MRI," *Magn. Reson. Med.*, vol. 42, no. 5, pp. 952-962, 1999.

[3] M. A. Griswold, P. M. Jakob, R. M. Heidemann, M. Nittka, V. Jellus, J. Wang, B. Kiefer, and A. Haase, "Generalized autocalibrating partially parallel acquisitions (GRAPPA)," *Magn. Reson. Med.*, vol. 47, no. 6, pp. 1202-1210, 2002.

[4] M. Lustig, D. Donoho and J. M. Pauly, "Sparse MRI: The application of compressed sensing for rapid MR imaging," *Magn. Reson. Med.*, vol. 58, no. 6, pp. 1182-1195, 2007.

[5] S. Wang, Z. Su, L. Ying, X. Peng, S. Zhu, F. Liang, D. Feng and D. Liang, "Accelerating magnetic resonance imaging via deep learning," Proc. of the 13th *International Symposium on Biomedical Imaging (ISBI)*, pp. 514-517, 2016.

[6] K. Hammernik, T. Klatzer, E. Kobler, M. P. Recht, D. K. Sodickson, T. Pock and F. Knoll, "Learning a variational network for reconstruction of accelerated MRI data," *Magn. Reson. Med.*, vol. 79, no.6, pp. 3055-3071, 2018.

[7] D. Lee, J. Yoo, S. Tak and J. C. Ye, "Deep Residual Learning for Accelerated MRI Using Magnitude and Phase Networks," *IEEE Trans. Biomed. Eng.*, vol. 65, no. 9, pp. 1985-1995, 2018.

[8] Y. Han, J. Yoo, H. H. Kim, H. J. Shin, K. Sung and J. C. Ye, "Deep learning with domain adaptation for accelerated projection-reconstruction MR," *Magn. Reson. Med.*, vol. 80, pp. 1189-1205, 2018.

[9] H. K. Aggarwal, M. P. Mani and M. Jacob, "MoDL: Model Based Deep Learning Architecture for Inverse Problems," *IEEE Trans. Med. Imaging*, vol. 38, no. 2, pp. 394-405, Feb. 2019.

[10] C. Qin, J. V. Hajnal, D. Rueckert, J. Schlemper, J. Caballero and A. N. Price, "Convolutional recurrent neural networks for dynamic MR image reconstruction," *IEEE Trans. Med. Imaging*, vol. 38, no. 1, pp. 280-290, Jan. 2019.

[11] J. Schlemper, J. Caballero, J. V. Hajnal, A. N. Price and D. Rueckert, "A deep cascade of convolutional neural networks for dynamic MR image reconstruction," *IEEE Trans. Med. Imag.*, vol. 37, pp. 491-503, 2018.

[12] K. Kwon, D. Kim and H. Park, "A parallel MR imaging method using multilayer perceptron," *Med. Phys.*, vol. 44, pp. 6209-6224, 2017.

[13] G. Yang, S. Yu, H. Dong, G. Slabaugh, P. L. Dragotti, X. Ye, F. Liu, S. Arridge, J. Keegan, Y. Guo and D. Firmin, "DAGAN: Deep De-Aliasing Generative Adversarial Networks for Fast Compressed Sensing MRI Reconstruction," IEEE *Trans. Med. Imag.*, vol. 37, pp. 1310–1321, 2018.

[14] C. M. Hyun, H. P. Kim, S. M. Lee, S. Lee and J. K. Seo, "Deep learning for undersampled MRI reconstruction," *Phys Med Biol*, vol. 63, no. 13, pp. 135007, 2018.

[15] T. Eo, Y. Jun, T. Kim, J. Jang, H. J. Lee and D. Hwang, "KIKI-net: cross-domain convolutional neural networks for reconstructing undersampled magnetic resonance images,"*Magn. Reson. Med.*, vol. 80, no. 5, pp.2188-2201, 2018.

[16] J. Y. Cheng, M. Mardani, M. T. Alley, J. M. Pauly and S. S. Vasanawala, "DeepSPIRiT: generalized parallel imaging using deep convolutional neural networks," Proc. of *the Joint Annual Meeting of ISMRM-ESMRMB*, pp. 570, 2018.

[17] S. U. H. Dar and T. Cukur, "Transfer learning for reconstruction of accelerated MRI acquisitions via neural networks." Proc. of the *26th Scientific Meeting of ISMRM,* 2018.

[18] Y. C. Eldar, A. O. Hero III, L. Deng, J. Fessler, J. Kovacevic, H. V. Poor et al, "Challenges and Open Problems in Signal Processing: Panel Discussion Summary from ICASSP 2017 [Panel and Forum]," *IEEE Signal Processing Mag,* vol. 34, no. 6, pp. 8–23, 2017.

[19] M. Akçakaya, S. Moeller, S. Weingärtner and K. Uğurbil, "Scan-specific Robust Artificial-neural-networks for k-space Interpolation-based (RAKI) Reconstruction: Database-free Deep Learning for Fast Imaging," *Magn. Reson. Med.*, vol. 81, no. 1, pp. 439-453, 2019.

[20] M. Barth, F. Breuer, P. J. Koopmans, D. G. Norris and B. A. Poser, "Simultaneous multislice (SMS) imaging techniques," *Magn. Reson. Med.*, vol. 75, no. 1, pp. 63-81, 2016.

[21] S. A. H. Hosseini, C. Zhang, K. Uğurbil, S. Moeller and M. Akçakaya, "sRAKI-RNN: accelerated MRI with scan-specific recurrent neural networks using densely connected blocks," Proc. of *Wavelets and Sparsity XVIII, International Society for Optics and Photonics,* vol. 11138, pp. 111381B, 2019.

[22] S. A. H. Hosseini, C. Zhang, S. Weingärtner, S. Moeller, M. Stuber, K. Uğurbil and M. Akçakaya, "Accelerated Coronary MRI with sRAKI: A Database-Free Self-Consistent Neural Network k-space Reconstruction for Arbitrary Undersampling," *arXiv preprint*, arXiv:1907.08137, 2019.

[23] F. Doshi-Velez and B. Kim, "Towards a rigorous science of interpretable machine learning," *arXiv preprint*, arXiv:1702.08608, 2017.

[24] W. Samek, T. Wiegand and K. R. Müller, "Explainable artificial intelligence: Understanding, visualizing and interpreting deep learning models," *arXiv preprint*, arXiv:1708.08296, 2017.

[25] K. He, X. Zhang, S. Ren, and J. Sun, "Deep residual learning for image recognition," Proc. of the 2016 *Conference on Computer Vision and Pattern Recognition (CVPR)*, pp. 770-778, IEEE, 2016.

[26] D. C. Van Essen, K. Ugurbil, E. Auerbach, D. Barch, T. E. J. Behrens, R. Bucholz, A. Chang, L. Chen, M. Corbetta, S. W. Curtiss, S. Della Penna, D. Feinberg, M. F. Glasser, N. Harel, A. C. Heath, L. Larson-Prior, D. Marcus, G. Michalareas, S. Moeller, R. Oostenveld, S. E. Petersen, F. Prior, B. L. Schlaggar, S. M. Smith, A. Z. Snyder, J. Xu, E. Yacoub and WU-Minn HCP Consortium, "The Human Connectome Project: a data acquisition perspective," *Neuroimage*, vol. 62, pp. 2222-2231, 2012.

[27] K. Setsompop, B. A. Gagoski, J. R. Polimeni, T. Witzel, V. J. Wedeen, and L. L. Wald, "Blipped-controlled aliasing in parallel imaging for simultaneous multislice echo planar imaging with reduced g-factor penalty," *Magn. Reson. Med.*, vol.67, no.5, pp. 1210-1224, 2012.

[28] S. Moeller, E. Yacoub, C. A. Olman, E. Auerbach, J. Strupp, N. Harel and K. Uğurbil, "Multiband multislice GE-EPI at 7 tesla, with 16-fold acceleration using partial parallel imaging with application to high spatial and temporal whole-brain fMRI," *Magn. Reson. Med.*, vol 63, no. 5, pp. 1144-1153, 2010.

[29] C. Zhang, S. Moeller, S. Weingärtner, K. Uğurbil and M. Akçakaya, "Accelerated Simultaneous Multi-Slice MRI using Subject-Specific Convolutional Neural Networks," Proc. of *52nd Asilomar Conference on Signals, Systems, and Computers*, pp. 1636-1640, IEEE, 2018.

[30] D. P. Kingma, and J. Ba, "Adam: A method for stochastic optimization," Proc. of *ICLR*, 2015.

[31] P. B. Roemer, W. A. Edelstein, C. E. Hayes, S. P. Souza and O. M. Mueller, "The NMR phased array," *Magn. Reson. Med.*, vol. 16, pp. 192-225, 1990.

[32] D. J. Larkman, J. V. Hajnal, A. H. Herlihy, G. A. Coutts, I. R. Young and G. Ehnholm, "Use of multicoil arrays for separation of signal from multiple slices simultaneously excited," *J. Magn. Reson. Img.*, 2001 Feb, vol. 13, no. 2, pp. 313-317, 2001.

[33] M. Weiger, K. P. Pruessmann and P. Boesiger, "2D SENSE for faster 3D MRI," *MAGMA*, vol 14, pp. 10-19, 2002.

[34] B. Zahneisen, T. Ernst and B. A. Poser, "SENSE and simultaneous multislice imaging," *Magn Reson Med* vol. 74, pp. 1356–1362, 2015.

[35] P. M. Robson, A. K. Grant, A. J. Madhuranthakam, R. Lattanzi, D. K. Sodickson and C. A. McKenzie, "Comprehensive quantification of signal-to-noise ratio and g-factor for image-based and k-space-based parallel imaging reconstructions," *Magn. Reson. Med.*, vol. 60, no.4, pp. 895-907, 2008.

[36] D. C. Van Essen, S. M. Smith, D. M. Barch, T. E. Behrens, E. Yacoub, K. Ugurbil and Wu-Minn HCP Consortium, "The WU-Minn human connectome project: an overview," *Neuroimage*, vol. 80, pp. 62-79, 2013.